11-22-2000

The Hall A Aerogel Čerenkov detector

Marius Coman
Florida International University

DOI: 10.25148/etd.FI14060885

FLORIDA INTERNATIONAL UNIVERSITY

Miami, Florida

THE HALL A AEROGEL ČERENKOV DETECTOR

A thesis submitted in partial fulfillment of the

requirements for the degree of

MASTER OF SCIENCE

in

PHYSICS

by

Marius Coman

2000

To: Dean Arthur W. Herriott
College of Arts and Sciences

This thesis, written by Marius Coman, and entitled The Hall A Aerogel Čerenkov Detector, having been approved in respect to style and intellectual content, is referred to you for judgment.

We have read this thesis and recommend that it be approved.

Werner U. Boeglin

Rudolf H. Fiebig

Sneh Gulati

Nongjian Tao

Pete E. C. Markowitz, Major Professor

Date of Defense: November 22, 2000

The thesis of Marius Coman is approved.

Dean Arthur W. Herriott
College of Arts and Sciences

Interim Dean Samuel S. Shapiro
Division of Graduate Studies

Florida International University, 2000

DEDICATION

Dedicated to my brother Emil N. Coman.

ACKNOWLEDGMENTS

This work would have not been possible without support from many people. First I would like to give special thanks to Dr. Pete E. C. Markowitz for his patience, encouragement, and advice throughout my graduate education. In addition, I would like to thank my committee members: Dr. Werner U. Boeglin, Dr. Rudolf H. Fiebig, Dr. Sneh Gulati and Dr. Nongjian Tao for their constructive criticism of my thesis.

I am very grateful to all the faculty and staff of the Florida International University Physics Department for their support in my education.

ABSTRACT OF THE THESIS

THE HALL A AEROGEL ČERENKOV DETECTOR

by

Marius Coman

Florida International University, 2000

Miami, Florida

Professor Pete E. C. Markowitz, Major Professor

The efficiency of the Aerogel Čerenkov detector for detecting particles having velocities greater than the speed of light in the aerogel media and the yield for rejecting particles having subthreshold velocities - smaller than the speed of light in the interaction media - was studied and is presented. The efficiency/inefficiency determination of the Aerogel Čerenkov detector consists of calculating the probabilities that a particle having a velocity above/below threshold generates a photoelectron in the aerogel block. The efficiency is determined using the normalised pulse height distribution of the photoelectrons. The Aerogel Čerenkov detector will play a key role in particle identification (PID) processes in Hall A at Jefferson Lab, allowing the separation of pseudoscalar mesons from pions which is required for many experiments to tag the flavor of the mesons and to identify the final states of interest for various experiments performed at Jefferson Lab.

TABLE OF CONTENTS

LIST OF TABLES

LIST OF FIGURES

1 Introduction

The development of particle identification (PID) detectors plays a key role in particle physics due to the complexity of the experiments. The identification of pseudoscalar mesons and distingushing such mesons from protons, neutrons and electrons is required for many experiments to determine the flavors (types) of the mesons (π, K) and to identify the final states of interest for specific experiments. A major requirement in particle physics experiments is to cleanly measure properties and interactions of these particles in order to test the validity of the reaction models.

This requirement implies an excellent charged hadron identification allowing, in this case, a good separation of pions and kaons up to momenta of 4 GeV/c and the ability to separate protons from kaons at similar momenta.

1.1 Particle Identification (PID) in Hall A

The kaon electroproduction experiments at Jefferson lab's Hall A can be conceptualized by the transfer of energy from an incident electron beam to the three constituent quarks in a proton or neutron (nucleon) target. The energy deposited into the target's nucleons causes one of the constituent quarks to be 'detached' from its quark partners. Two new exotic quarks are pulled from the quark sea (vacuum sea), a 'strange' quark and a 'strange' antiquark. The strange antiquark and the detached quark form a detectable kaon. Kaons detected at Jefferson Lab can give an insight of how quarks are created out of energy, and about how antimatter is produced. This requires a good identification of the particles involved as well as a separation between the par-

ticles subject to study and the contaminating background particles. The problem examined in this thesis is to determine the efficiency of a diffusion Aerogel [1] detector for hadrons [2] and the related rejection factor for sub-threshold background particles . The study was done as part of the experimental program to measure kaons, members of the pseudoscalar meson octet (along with the π and an η) in Hall A at Jefferson Lab using a threshold Čerenkov particle identification detector.

The primary aim of this research project was to study the number of photoelectrons [3] generated in the Aerogel detector when detecting particles whose velocities are greater than the speed of light in the aerogel medium and the yield (light gain)[4] for rejecting particles with velocities smaller than the speed of light in the interaction medium.

A secondary problem presented is how to determine the best thickness of aerogel [5]that allows the greatest detection efficiency for particles of interest and greatest rejection factor for the contaminating particles.

Another facet of the 'best thickness' problem will be presented.It consists of determining the extent to which the aerogel thickness has an influence on the detection efficiency and the rejection factor, given that a thicker aerogel will generate more photons. Although a thicker radiator generates more photons, the short scattering length of the aerogel prevents them from reaching the detector's photomultipliers.

[1]The aerogel is a transparent, highly porous material of low density (0.05 – 0.15 g/cm^3)

[2]Hadrons can be classified in two groups: the *baryons*, fermions with half-integral spin, and the *mesons*, bosons with integral spin

[3]The photons converted into electrons, making use of the photoelectric effect

[4]The energy loss of a charged particle in a scintillation counter that is converted into visible light

[5]The medium for the production of Čerenkov radiation

The results of this study will facilitate the particle identification in Hall A at Jefferson Lab, allowing further studies on electromagnetic kaon electroproduction.

2 Aerogel Čerenkov detector's working principle

2.1 Čerenkov radiation

2.1.1 Interaction of radiation with the aerogel media

The aerogel Čerenkov detector, as its name suggests, functions based on the production and detection of Čerenkov radiation in the aerogel medium. The physical process that enables us to detect the particles involved in an electroproduction experiment such as the H(e,e'K)Y (with Y being the Λ or the Σ hyperons) inelastic reactions is the electromagnetic interaction between the charged particles and the aerogel medium. The charged particles can be directly detected through their electromagnetic interactions with the atomic electrons of the detector radiator – the aerogel. In general when a charged particle crosses a layer of material, three processes can occur: the material's atoms can be ionized, the particle can emit Čerenkov radiation or the particle can generate the emission of transition radiation.

When a charged particle has a velocity greater than the local phase velocity of light it emits a characterictic cone of radiation (Čerenkov radiation). The charged particle also radiates when crossing suddenly from one medium to another with different optical properties (transition radiation). These two processes are not important from the point of view of the energy loss, but both processes are used in high-energy physics detectors.

In the electromagnetic interaction of a charged particle of mass m and velocity v in a material of refractive index n and with dielectric constant:

$$\epsilon = \epsilon_1 + i\epsilon_2 \tag{1}$$

such that $\epsilon_1 = n^2$, a photon of energy $\hbar\omega$ and momentum $\hbar k$ is created if $v > c/n$. From the energy-momentum conservation the relation between the four-momentum of the incoming particle p (a charged particle -pion, electron, proton or kaon), the four-momentum p' of the outgoing particle, and the photon momentum p_γ is inferred:

$$p' = p - p_\gamma \tag{2}$$

For small photon energies,

$$\hbar\omega << \gamma mc^2 \tag{3}$$

with $\gamma = \sqrt{\frac{1}{1-\beta^2}}$ the relativistiv factor of the incoming particle, $\beta = v/c$ and m its mass. The equation (2) gives [6]:

$$\omega = vkcos\theta_c \tag{4}$$

where θ_c is the angle between the directions of the emitted photon and the incoming particle. In the radiator material the photon energy and momentum are related by the dispersion relation:

$$\epsilon\omega^2 = k^2c^2 \tag{5}$$

From these two equations Eqs. (4) and (5) we can deduce that:

$$cos\theta_c\sqrt{\epsilon}\frac{v}{c} = 1 \tag{6}$$

At photon energies below the excitation energies of the aerogel (the so called 'optical region') the dielectric constant is a real number greater than 1, so the angle θ_c at

[6]Konrad Kleinknecht, Detectors for particle radiation, Cambridge Univ. Press, 1998

which the radiation is emitted is also real, ($|cos\theta_c| < 1$), for particle velocities greater than the ratio between the speed of light and the dielectric constant (phase velocity):

$$v > \frac{c}{\sqrt{\epsilon}} \tag{7}$$

The Čerenkov effect, the emission of real photons, does occur if the velocity of the particle is larger than the phase velocity $\frac{c}{\sqrt{\epsilon}}$ of light in the aerogel material (the 'Čerenkov threshold'). For certain photon energies in the range from 2eV through 5 keV, only virtual photons are exchanged between the particle and the atoms of the radiator (aerogel - in our case), resulting in excitation or ionization of the aerogel's atoms and a corresponding energy loss of the particle.

At photon energies above 5 keV (the X-ray domain), the absorption coefficient becomes small and the threshold velocity for the Čerenkov effect is then larger than the velocity of light in vacuum and transition radiation does occur. Transition radiation can still be emitted below this threshold if there are discontinuities in the aerogel material traversed by the particle.

The production of Čerenkov radiation can be deduced from the formula for the differential cross section per electron and per energy loss in the photoabsorbtion model, considering only the photon energies below the excitation energy of the atom (i.e., in the optical region) where the cross section for the absorption of a photon of energy E by the aerogel's atoms vanishes):

$$\frac{d\sigma}{dE} = \frac{2\alpha}{\beta^2 ZNhc}\left(\beta^2 - \frac{\epsilon_1}{\epsilon^2}\right)\theta \tag{8}$$

Here $\alpha = \frac{1}{137}$ is the fine structure constant, β is the ratio between the particle velocity and the speed of light, $\epsilon = \epsilon_1 + i\epsilon_2$ is the complex dielectric constant of the aerogel

(crossed media), see eq. (1),

$$N = \frac{\rho N_A}{A} \tag{9}$$

is the atomic density, ρ is the aerogel density, A is the atomic mass number, N_A is the Avogadro number and θ is the phase of the complex expression:

$$1 - \epsilon_1\beta^2 + i\epsilon_2\beta^2 = ae^{i\theta} \tag{10}$$

In the above formula we considered the photon energies below the excitation energy of the aerogel atoms so σ_γ, the cross-section for absorption of a photon of energy E by the atoms of the medium was neglected. In the optical region, where the photon energies are below the excitation energy of the aerogel atoms, $\epsilon_2 = 0$ and $\epsilon_1 = \epsilon$, such that the phase θ of the expression $1 - \epsilon_1\beta^2$ vanishes below the Čerenkov threshold

$$\beta^2 = \frac{1}{\epsilon_1} \tag{11}$$

and jumps to π above the threshold. The flux of photons in the energy interval $dE = \hbar\omega$ from a path length L of the charged particle in the aerogel medium is obtained by multiplying the equation (8) by the density of electrons, above the threshold [7]:

$$\frac{dn}{d\omega} = \frac{\alpha}{c}\left(1 - \frac{1}{\beta^2\epsilon}\right)L \tag{12}$$

For an aerogel length much greater than the wavelength of radiation emitted, $L >> \lambda$, the above formula gives the intensity of the Čerenkov radiation. The classical theory of the Čerenkov effect attributes this electromagnetic radiation to the asymmetric polarization of the medium in front of and behind the charged particle, representing

[7] J. D. Jackson, Classical Electrodynamics, Wiley, New York, 1996

a net electric dipole moment varying with time. In the same way as for an acoustical shock wave generated by a body moving with supersonic velocity, the Čerenkov wave front can be constructed by the superposition of spherical elementary Huygens waves produced by the particle along its trajectory. During the time interval t the wave travels a distance tc/n, and the particle moves a distance $t\beta c$. From these two distances the direction of propagation of the Čerenkov wave is obtained:

$$cos\theta_c = \frac{ct}{n\beta ct} = \frac{1}{\beta n} \tag{13}$$

with θ_c the angle of the Čerenkov radiation emitted relative to the particle trajectory. The angle of emission of Čerenkov radiation produced by a particle which crosses a medium with a velocity βc with index of refraction n is

$$\theta_c = cos^{-1}(n\beta)^{-1} \tag{14}$$

and in the case of small angles:

$$\theta_c = \sqrt{2\left(1 - \frac{1}{n\beta}\right)} \tag{15}$$

This radiation is, therefore, only emitted if $\beta > 1/n$. The minimal velocity $vt = c/n$ at which Cherenkov emission takes place is called the threshold velocity; the angle θc is called the Čerenkov angle. The types of detectors which rely on the particles' detection depending on their velocity are called threshold Čerenkov counters. Ideally the threshold Čerenkov counters have a binary response to particles, i.e. they 'fire'[8], or not depending on the incident's particle velocity above or below threshold. Figure 1 shows the values of the Čerenkov angle θ_c as a function of particle velocity for two different aerogels with different refractive indexes n.

[8] i.e. light is emitted

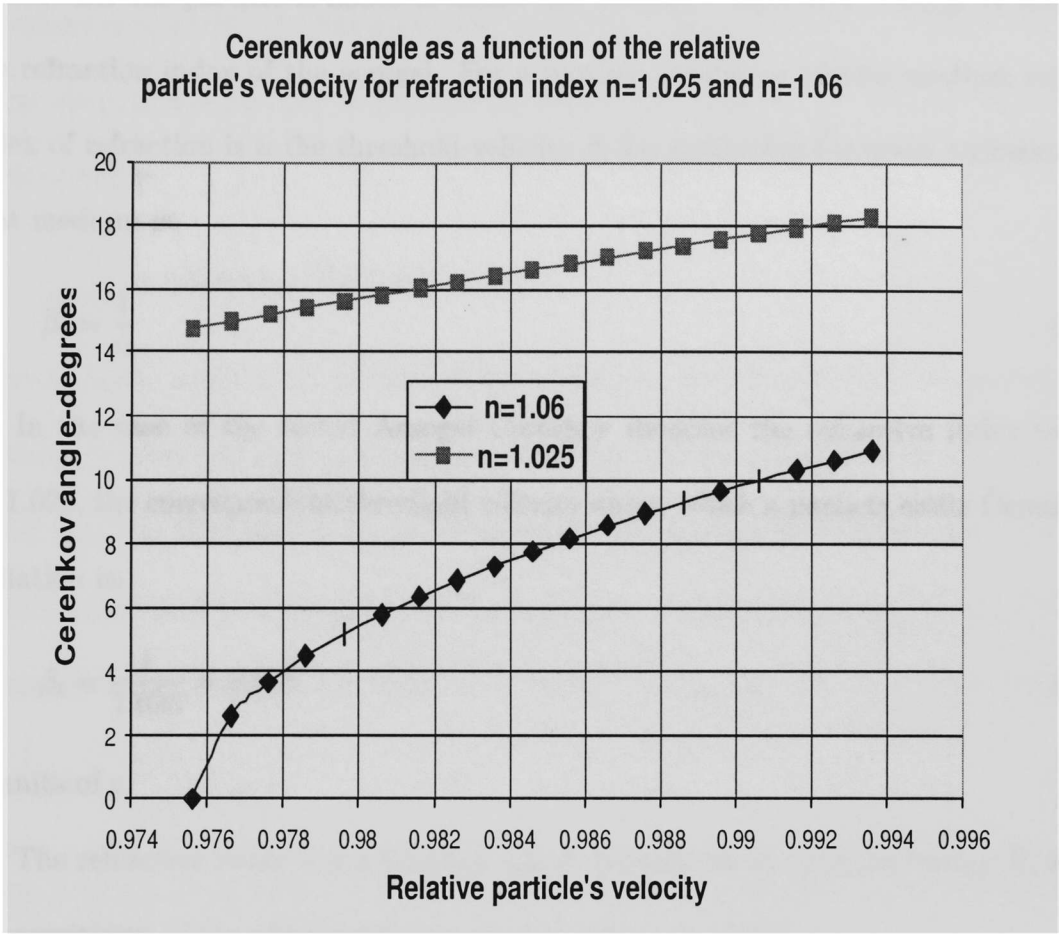

Figure 1: Čerenkov angle θ_c as a function of particle velocity for different values of the refractive index n

The threshold Čerenkov detector working principle is based on the properties of Čerenkov radiation namely the existence of a threshold velocity for producing the radiation in the propagation media, the dependence of the Čerenkov radiation emission angle θ_c on the velocity of the particle and the dependence of the number of emitted photons on the particle's velocity. For different particular experimental applications the Čerenkov radiation emission angle θ_c, the number of emitted photons and threshold velocity can be tuned by modifying the refractive index n of the propagation media. The Čerenkov threshold detectors distinguish between charged particles based

on whether the particle is above or below the Čerenkov threshold velocity β_t with n the refraction index of the aerogel. For a particle crossing a certain medium whose index of refraction is n the threshold velocity β_t for producing Čerenkov radiation in that medium is:

$$\beta_t = \frac{1}{n} \tag{16}$$

In the case of the tested Aerogel Čerenkov detector the refractive index being n=1.025, the correspondent threshold velocity above which a particle emits Čerenkov radiation is:

$$\beta_t = \frac{1}{1.025} = 0.975 \tag{17}$$

in units of c.

The refractive index n is a function which depends on the photon energy E, as is the sensitivity of the photomultiplier used to detect the light.

2.1.2 Number of photons generated in the aerogel

An accurate identification of the particles that give a signal in the Aerogel Čerenkov detector depends on the number of photons generated in the aerogel media, due to the charged particle interaction with the aerogel atoms. The number of photons produced by a particle with charge Ze passing a length x of aerogel material (per differential path length and energy interval of the photons) can be written [9]:

$$\frac{d^2N}{dEdx} = \frac{\alpha Z^2}{\hbar c} sin^2\theta_c = \frac{\alpha^2 Z^2}{r_e m_e c^2}\left(1 - \frac{1}{\beta^2(E)}\right) \tag{18}$$

[9]Review of Particle Physics, C, Vol. 15, Springer, 2000

where $\alpha \simeq 1/137$, the fine structure constant. Using $\alpha^2/r_e m_e c^2 = 370 cm^{-1} eV - 1$ for an electron the number of photons produced by a unit charge particle (electrons in our case) is:

$$\frac{d^2N}{dEdx} \simeq 370 sin^2\theta_c(E) eV cm^{-1} \tag{19}$$

where θ_c is the angle made by the emitted radiation with the direction of the moving particle. A more detailed consideration of the process for radiators of finite length L shows that the Čerenkov radiation is emitted with an intensity distribution peaked around an angle θ_c, caused by diffraction effects [1]. The intensity distribution has a maximum at: $\theta = \theta_c$, and the distance between consecutive diffraction maxima is [2]:

$$\Delta\theta = \left(\frac{\lambda}{L}\right) sin\theta_c \tag{20}$$

where λ is the wavelength of the Čerenkov light. So the number of photons emitted per differential wavelength interval and differential angular interval is [11]:

$$\frac{d^2N}{d\lambda dcos\theta} = \frac{2\pi\alpha}{\lambda}\left(\frac{L}{\lambda}\right)^2\left(\frac{sinx}{x}\right)^2 sin^2\theta \tag{21}$$

where

$$x(\theta) = \left(\frac{1}{n\beta} - cos\theta\right)\frac{\pi L}{\lambda}. \tag{22}$$

In the limiting case of very thick aerogel acting as radiator ($L >> \lambda$), the function

$$\left(\frac{L}{\lambda}\right)^2\left(\frac{sinx}{x}\right)^2 \tag{23}$$

[1] J.D. Jackson, Classical Electrodynamics, Wiley, New York (1966)

[2] Konrad Kleinknecht, Detectors for particle radiation, Cambridge Univ. Press, 1998

becomes proportional to a δ function at $x = 0$ and after angular integration the number of photons becomes [11]:

$$\frac{dN}{d\lambda} = \frac{2\pi\alpha}{\lambda^2} L sin^2\theta \tag{24}$$

Integrating over the wavelength the number of photons emitted in the wavelength interval from λ_1 to λ_2 then is:

$$N = 2\pi\alpha L \int_{\lambda_1}^{\lambda_2} \frac{sin^2\theta_c}{\lambda^2} d\lambda. \tag{25}$$

In the case of the Aerogel Čerenkov detector taking into account the photomultiplier tubes needed to detect the Čerenkov radiation, the eq. (25) must be multiplied by the the PMT's (photomultipliers') response function (sensitivity) and integrated over the region for which the product between the relative velocity of the particle and the index of refraction is smaller than 1, that is $\beta n(E) < 1$. The number of photoelectrons (p.e.'s) detected in the photomultipliers depends on the path length L, in the aerogel media, the efficiency ϵ_{coll} for collecting the Čerenkov light (depending on the detector's design a typical collection efficiency of 90 % can be achieved) and the quantum efficiency ϵ_{det} [3] of the phototubes (in our case Burle 8854). The quantum efficiencies for the Burle photomultipliers was determined prior to these calculations and is discussed in detail in section 2.2.3.

Thus one obtains the number of photoelectrons [4]:

$$N_{p.e.} = L \frac{\alpha^2 z^2}{r_e m_e c^2} \int \epsilon_{coll}(E)\epsilon_{det}(E) sin^2\theta_c(E) dE \tag{26}$$

[3]The ratio of the numbers of photoelectrons emitted to the number of incident photons

[4]Review of Particle Physics, C, Vol. 15, Springer, 2000

The functions ϵ_{coll} - the efficiency for collecting the Čerenkov light, ϵ_{det} - the quantum efficiency of the phototubes and θ_c - the Čerenkov radiation emission angle, all depend on the photon energy E, although in some specific detectors θ_c (or, equivalently, the index of refraction) can be constant over the useful range of photocathode sensitivity. When the angle of emmission for Čerenkov radiation is constant over the range of photocathode sensitivity the number of photoelectrons that get detected are given by [5]:

$$N_{p.e.} = L\frac{\alpha^2 z^2}{r_e m_e c^2}\langle sin^2\theta_c\rangle \int \epsilon_{coll}(E)\epsilon_{det}(E)dE \tag{27}$$

In our detector we used Burle photomultipliers and the overall detection efficiency (integrated over the energy range) for a Burle PMT is [15]

$$\int \epsilon_{det}(E)dE \simeq 0.27 \tag{28}$$

Thus the number of photoelectrons expected to be produced per unit path length of aerogel as a function of the emission angle considering an achievable efficiency for collecting the Čerenkov light $\langle\epsilon_{coll}\rangle \simeq$ of 90 % are:

$$\frac{N_{p.e.}}{L} \simeq 96.3\langle sin^2\theta_c\rangle cm^{-1} \tag{29}$$

for particles having the atomic number $z = 1$.

The length L of Čerenkov threshold detectors needed for separation of particles of momentum p increases as momentum squared, p^2. We want to distinguish between two types of particles π and K with masses m_π=139.567 MeV/c^2 and m_K=493.7 MeV/c^2 (obviously $m_\pi < m_K$). Then the refractive index of the radiator can be

[5]Review of Particle Physics, C, Vol. 15, Springer, 2000

chosen such that the heavier particle with mass m_p does not yet radiate, or is just below the threshold, $\beta = 1/n$ and

$$n^2 = \frac{\gamma_2^2}{\gamma_2^2 - 1}. \tag{30}$$

where γ is the relativistic factor:

$$\gamma_t = \sqrt{\frac{1}{1 - \beta_t^2}} = 1 \tag{31}$$

An empirical formula for calculating the expected number of photoelectrons produced in the aerogel Čerenkov detector considering the refraction index and the reflectivity of the walls is[6]:

$$N_{p.e.} = \frac{n^2 - 1}{n^2} LK \frac{\epsilon}{1 - \eta(1 - \epsilon)} \tag{32}$$

where n=1.025 is the refraction index of the aerogel, L is the length of the aerogel, K is an empirical factor which takes into account the type of PMTs used for detecting the Čerenkov radiation, ϵ is the fraction of total area covered by the PMTs and η the reflectivity of the walls. In our case the fraction of total area covered by the PMTs is

$$\epsilon = \frac{A_{tot}^{diff+tray}}{A_{tot}^{PMT}} = \frac{A_{diff} + A_{tray}}{A_{tot}^{PMT}} = \tag{33}$$

$$= \frac{lw_{diff} + lw_{tray} + lh_{diff} + lh_{tray} + 2wh_{diff} + 2wh_{tray}}{24 A_{PMT}} = 12.3\%$$

where A_{tot}^{PMT} is the total active area of the photomultipliers, A_{diff},A_{tray} are the areas of the diffusion box and aerogel tray, l is the length of the aerogel tray and diffusion box, w_{diff}, w_{tray} are the widths of the diffusion box and aerogel tray, h_{diff} and h_{tray} are the heights of the diffusion box and aerogel tray. The quantity A_{PMT}

[6]P. Carlson et al., Nuclear Instruments and Methods 160/1979

represents the active area of the Burle PMT. Plugging in the values in formula (33) we obtained for the number of expected photoelectrons for the aerogel thicknesses of 9 and 3 cm:

$$N_{p.e.-3cm} = 4.2 \tag{34}$$

$$N_{p.e.-9cm} = 12.9$$

For the calculation we used $K = 27cm^{-1}$ [7] and the reflectivity of the walls (aerogel tray and diffusion box were covered with millipore paper) was $\epsilon = 97\%$.

This is the expected number of photoelectrons produced per unit path length considering good optical properties of the aerogel. Separation of two kinds of charged particles with different masses, m_1 and m_2, with a Čerenkov counter of fixed length L is only possible up to a relative maximum momentum of the particles; for threshold counters this limiting momentum P_{max} can be inferred from the following eq [8]:

$$\sin^2_{\theta_c} \simeq \frac{c^2(m_2^2 - m_1^2)}{p_2} \tag{35}$$

The equation is valid when the relativistic factor is much grater than 1:

$$\gamma = \sqrt{\frac{1}{1-\beta_t^2}} >> 1.$$

The relevant value is the number of photons N emitted by the particles above threshold velocity with mass m_1, if the slower ones having mass m_2 does not radiate at that

[7] P. Carlson et al., Nuclear Instruments and Methods 160/1979

[8] Konrad Kleinknecht, Detectors for particle radiation, Cambridge Univ. Press, 1998

time, i.e. it is just below the Čerenkov threshold. Since the valuie of

$$\frac{N}{L} = Asin^2\theta_c \frac{photons}{cm}$$

is determined by the Čerenkov angle for the faster particle (A is a parameter that depends on the wavelength range where the photomultiplier's photocathode is sensitive). According to eq. (35) $sin\theta_c$ drops linearly with $1/P$. The threshold velocity at which a charged particle can produce the number of photoelectrons per unit length given in equation (29) and the threshold momenta [9] for protons, kaons and pions are given in Table 1.

β_t	p_p (MeV/c)	p_K (MeV/c)	p_π (MeV/c)
0.9756	4170.098	2193.982	620.298

Table 1: Threshold momenta for protons, kaons and pions

Velocities (relative to the speed of light) of three types of particles (particles of interest in Kaon electroproduction experiments,) protons , kaons, and pions, as a function of particles' momenta, are shown in Fig. 2.

The Aerogel Čerenkov detector was designed to be used for experiments where the separation of kaons from pions is necessary in a momentum range from 0.5 GeV/c to 2.5 GeV/c. The overall efficiency [10] of the Aerogel Čerenkov detector is determined by Poisson fluctuations. Their influence is critical for separation of particles when one type of particle is dominant.

[9] Momenta above which the particles produce Čerenkov radiation

[10] The fraction of the particles that gave a signal in the detector and those that hit the detector

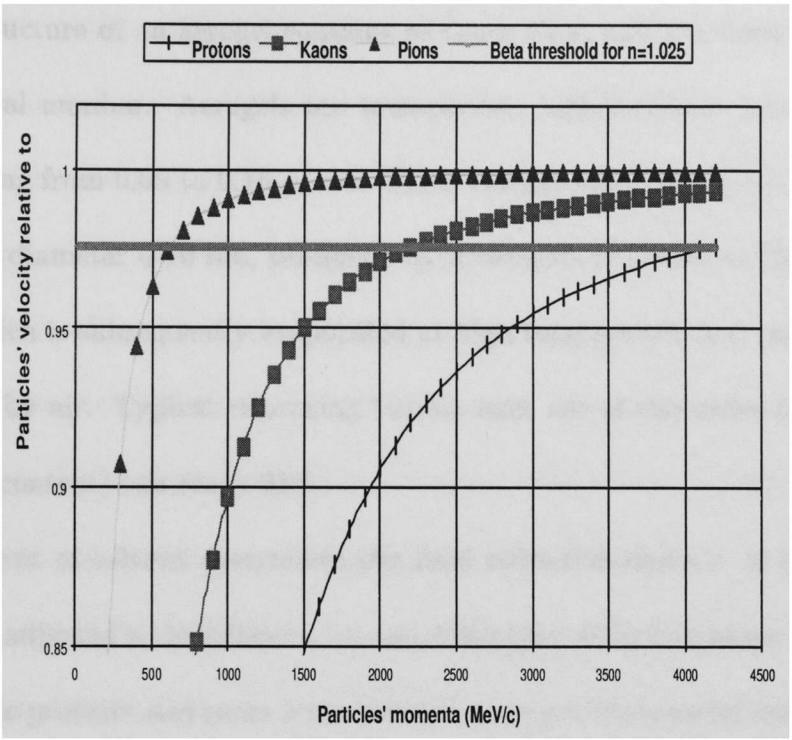

Figure 2: Particle velocities as a function of particles' momentum; Threshold velocity for aerogel index n=1.025

2.2 Aerogel Detector Components

2.2.1 Aerogel properties

The Aerogel Čerenkov detector has three main components: the diffusion box (whose main purpose is to diffusely reflect the Čerenkov radiation produced in the aerogel media), the radiator [20] located in a tray, and the photomultipliers whose purpose is to detect the emitted Čerenkov radiation. The components and the properties of the Aerogel detector will be discussed in detail in the next section. The medium used as

[20]The aerogel media that produces the Čerenkov radiation

radiator in the Čerenkov detector was the aerogel with refraction index n=1.025. The molecular structure of an aerogel contains m times SiO_2 and $2m$ times H_2O, where m is a natural number. Aerogels are transparent, highly porous materials of low density ranging from 0.05 to 0.15 g/cm^3. Silica aerogel consists of amorphous grains of silica with diameter 4-10 nm, produced by hydrolysis of Silane in the presence of a solvent, which is subsequently evaporated at high temperature and under pressure, i.e. replaced by air. Typical remaining bubble sizes are of the order of 60 nm; the porosity (air content) can reach 98%.

The amount of solvent determines the final refractive index n of silica aerogel, which can be adjusted to be between 1.2 and 1.002 (the refractive index of light gases at atmospheric pressure and room temperature). Aerogel thus can be used for particle identification by Čerenkov radiation in the momentum range of a few GeV/c.

The measurements of the aerogel's refractive index is expected to obey the formula of Clausius-Mosotti [21]:

$$n - 1 = (0.2100 \pm 0.001)\rho \tag{36}$$

where ρ is the density of the material.

The homogeneity of the gel influences the optical quality of the aerogel. For pores larger than 20 % of the wavelength of radiated light, Rayleigh scattering will affect the light transmission. Absorption effects dominate at $\lambda \leq 250$ nm. At λ=400 nm, the diffusion length is of the order of 10 mm. The directionality of the radiated Čerenkov light is also affected by Rayleigh scattering [22], and the use of the mirror

[21] Arlon J.Hunt, Aerogel optical properties and spectrum, http://rd11.web.cern.ch/RD11

[22] By diminishing the Čerenkov radiation

focusing technique for light collection becomes difficult.

The process of light diffusion in the walls surrounding the radiator can be used for light collection in these cases and a high collection efficiency can be achieved depending on the diffusive reflection coefficient. The interaction of light with the inhomogeneities in the aerogel material produces the scattering of the light. A single large molecule (with an inherent inhomogenity) of the aerogel or some clusters of small non-uniform molecules may cause the scattering of the radiation. The scattering process becomes more effective if the size of the scattering center (molecule or cluster) is comparable to the wavelength of the incident light. It means for visible light, for scattering to occur, the size (diameter) of the scattering center should be about $d \simeq$400-700 nm.

When scattering centers are smaller in size than the wavelength of the incident light, scattering is much less effective. In silica aerogels, the primary particles have a diameter of $\sim$2-5 nm, and do not contribute significantly to the light scattering process. In silica aerogels there is a network of pores which can act as scattering centers. The majority of these pores, that act as scattering centers, are much smaller ($\sim$20 nm) than the wavelength of visible light.

Because the scattering efficiency depends on the size of the scattering center, radiations having different wavelengths will scatter with varying magnitudes. This causes the blue appearance of the reflected light off silica aerogels [23].

A determination of the relative contributions of Rayleigh scattering and the wavelength-independent transmission factor (due to surface damage and imperfec-

[23]Red light is scattered less by the fine structure of aerogels because it has a longer wavelength

tions) for silica aerogel can be done by measuring the transmission spectrum of an aerogel of known thickness, and by plotting the transmission factor versus the inverse fourth power of the wavelength. These data of the transmission factor are fit to the equation[24]:

$$T = Ae^{(\frac{-IL}{\lambda^4})} \tag{37}$$

where T is the transmittance coefficient, A is a transmission factor which is independent of the wavelength, I is the intensity of Rayleigh scattering, L is the aerogel thickness, and λ is the wavelength of the radiation. The parameters A and I are an indication of the aerogel transparency[25]. The scattering process may also be accompanied by absorbtion which will further attenuate the transmitted light. The aerogel Čerenkov detector uses a diffusion box for the reflection of the Čerenkov radiation produced when the charged particles passes through the aerogel. The diffusive box, coated with Millipore paper backed up by regular paper, ensures a high collection efficiency due to a 0.97 reflection coefficient. The light collection efficiency of a large diffusing box is lower than the one obtained with a focusing system (mirrors) but diffused light as well as direct light is collected so that the usable aerogel thickness is no longer limited by the absorption length which is considerable [26].

[24] Arlon J.Hunt, Aerogel optical properties and spectrum

[25] Aerogels with a high value of A and a low value of I will be the most transparent

[26] Jim Napolitano, Thomas Jefferson National Lab., technical report

2.2.2 Photomultipliers characteristics

The photomultipliers (PMT) used to detect the Čerenkov radiation were Burle 8854. This is a 129 mm (5 inch) diameter PMT with ultraviolet-Transmitting Glass Window. The Burle 8854 phototube is a 14 stage head on photo-multiplier having a bialkali photocathode of high quantum efficiency and an extremely high gain cesiated gallium phosphide first dynode followed by high stability copper beryllium dynodes in the succeeding stages. The high gain first dynode permits the direct observation of peaks corresponding to one two and three photoelectrons. According to the manufacturer the photomultipliers' features are[27]:

1. High quantum efficiency (0.225 at λ=385 nm);
2. Ultraviolet response to 220 nm;
3. Low Dark Noise at 22 degrees C;
4. Dark Pulse Summation;
5. SIGMA approximate 1000 counts per second;
6. Time Resolution Characteristics:
7. Anode-Pulse Rise Time - 2.9 x 10^{-9}s at 3000 V;
8. Electron Transit Time - 6.6 x 10^{-8}s at 3000 V;
9. Spectral Response 220 - 660 nm.

[27]BURLE TECHNOLOGIES, INC., http://www.burle.com

The dynode amplification chain also incorporates a resistor in series with the metallic shield to eliminate the possibility of electric shock through careless handling; this high impedance also limits the current leak, in the unlikely event of a complete dielectric breakdown between the shields and the aluminum parts of the detector.

2.2.3 Photomultipliers' quantum efficiencies

The Burle phototubes were studied and their quantum efficiency determined prior to the installation in the Aerogel Čerenkov detector. The testing equipment used for the determination of PMT's quantum efficiency included the following modules and devices:

1. Support structure for assembly consisting of a light emitting diode (LED) and PMT;
2. Pulse Generator (HP8013A) for powering LED diode;
3. Nuclear Instruments and Methods (NIM) crate with electronics module;
4. CAMAC [28] crate with readout crate controller (Sparrow SCM 301);
5. High Voltage power supply (LeCroy 1458);
6. SCA module (scalers);
7. Analog to digital converter (ADC) module;
8. Aquisition card and analysis system computer (Macintosh).

[28] A modular data aqusition system

The support structure consisted of two brass tubes, one inserted into the other. The inner tube can be moved inside of the external tube in the longitudinal direction, for easy replacement of PMTs. The PMT installed into the inner tube is surrounded by a high magnetic permeability shielding. One end of the inner tube had a voltage divider and signal connectors for the PMT, while at the other end was mounted an LED diode.

The triggering pulse was sent to the LED from a pulse generator with an amplitude of 5.80 Volts and the width of 60 ns. The LED diode produced short (~10ns) blue light flashes. Three layers of Kodak filters were installed between the PMT and the LED, to adjust the quantity of light that gets into the photo-tube. Each of the filters contributed with an attenuation factor of 4.5. We used the filter layers in front of the LED as an alternative to attenuating the electric signal which could have caused an instability of the LED. The electronics schematic used for determining the PMT's quantum efficiencies is present in Fig. 3.

The signal from PMT was sent to the discriminator [29] module (Phillips 708) through a linear Fan/In/Fan/Out module (LeCroy 428F). The threshold of the discriminator was set to $\sim$ 30mV. From the discriminator module the signal was sent through a gate generator and a delay line (150 ns) to an Analog to Digital Converter [30] (ADC) [31]. A copy of the output signal of the discriminator was sent to a channel of a scaler module. The synchronous pulse from the pulse generator (HP-8013A) was

[29] Generates precise logic pulses in response to its input that exceeds a given threshold

[30] Measure the charge or the voltage of an input signal and produce a digital signal proportional with it

[31] LeCroy 2249W; www.lecroy.com

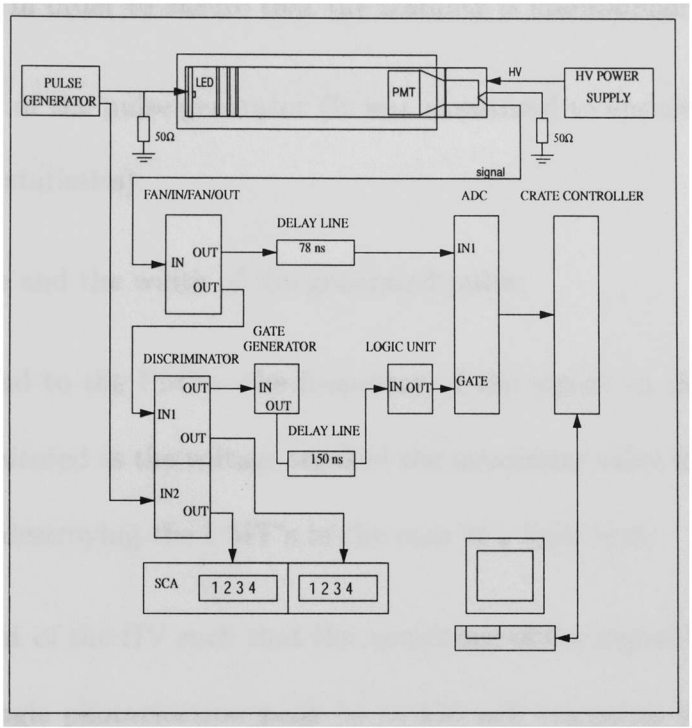

Figure 3: Scheme showing the interconnection between electronic modules used for determining the PMT's quantum efficiencies

sent through the discriminator module to the gate generator (LeCroy 222) in order to form a gate ($\sim$ 100ns). Also from the output of the disriminator the synchronous pulse was sent to another channel of the scaler module.

The readout controller was used to transfer data from the ADC to the aquisition card located in to the computer. The 'KMAX'[32] software was used for data acquisition and ADC spectra preview. The rate of the background events (measured by unplugging the LED) and the total rate recorded by the ADC (measured connecting

[32]Sparrow Corporation, www.sparrowcorp.com

the LED) were determined by using the scalers. For each measurement the following items were checked in order to ensure that the stability is maintained:

1. the frequency of the pulse generator (It was monitored to ensure its constancy in within the statistics);
2. the amplitude and the width of the generated pulse;
3. the HV applied to the PMTs -the frequency of the signal on the SCA (count rate) was monitored as the voltage reached the maximum value to eliminate the possibility of destroying the PMT's in the case of a light leak;
4. the adjustment of the HV such that the amplitude of the signal from the PMT due to the single photoelectron peak be at 150 mV (ensuring in this way the same gain for all the PMT's);
5. the variations of the PMT's count rate in time;
6. the possible light leaks.

The following data for each PMT were recorded:

1. PMT's serial number;
2. PMT's operating HV;
3. The width, amplitude and frequency of the pulse generator;
4. The noise count rate and total count rate;
5. The threshold of the discriminator.

The data acquisition was started after the above items were checked. A couple of measurements for the same PMTs were performed to estimate the systematic errors. The data were analyzed by using the Physics Analysis Workstation (PAW)[33] package. A typical ADC spectra [34] from a Burle PMT is presented on Fig. 4.

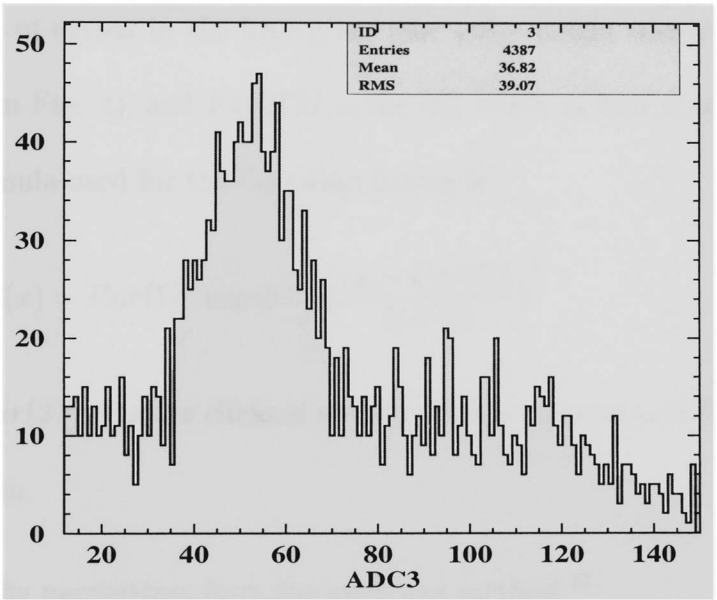

Figure 4: ADC spectra from a Burle PMT – on the y axis is represented the number of counts versus the ADC pulse height

The quantum efficiency Q_e [35] of the PMT was calculated by two methods:

[33]CERN-European Laboratory for Particle Physics, http://wwwinfo.cern.ch

[34]The pulse height distribution of the Analog to digital converter

[35]The ratio of the numbers of photoelectrons emitted to the number of incident photons

1. Using the parameters from a Gaussian fitting [36]of the ADC spectra; the Gaussian fit is a good aproximation since we are not interested in the standard deviation but in the mean of the distribution

$$Q_e = \frac{FWHM \times Par(1)}{N_t} \tag{38}$$

where $Par(1)$ is the height of the peak from the Gaussian fit, N_t is the total number of events in the histogram (the pulse height distribution of the PMT shown in Fig. 4), and $FWHM$ is the full width at half maximum of the peak; the formula used for the Gaussian fitting is:

$$G(x) = Par(1) \cdot \exp(0.5 \cdot (\frac{(x - Par(2))}{Par(3)})^2 \tag{39}$$

with $Par(2)$ being the channel number with maximum and $Par(3)$ the standard deviation.

2. Using the parameters from the sweeping method [37]:

$$Q_e = \frac{\sum_{i=N_{first}}^{N_{last}} N_i}{N_t} \tag{40}$$

where N_t is the total number of events in the histogram, N_i the number of events in the i-th channel, N_{first} number of start channel for summing, N_{last} number of last channel considered for summing. The result of fitting the ADC spectra from a Burle

[36]We started the Gaussian fit from a higher ADC channel to disregard the noise due to the low charge events that appears on the left side of the pulse height distribution

[37]The sweeping method was done using PAW software to calculate the area under the histogram within the specified limits and the average

PMT with a Gaussian distribution function [38] – fitting used to determine the PMT quantum efficiency –is presented in Fig. 5. The tail on the left of the ADC pulse height distribution is due to the low charge events and the one on the right of the distribution is due to background events[39].

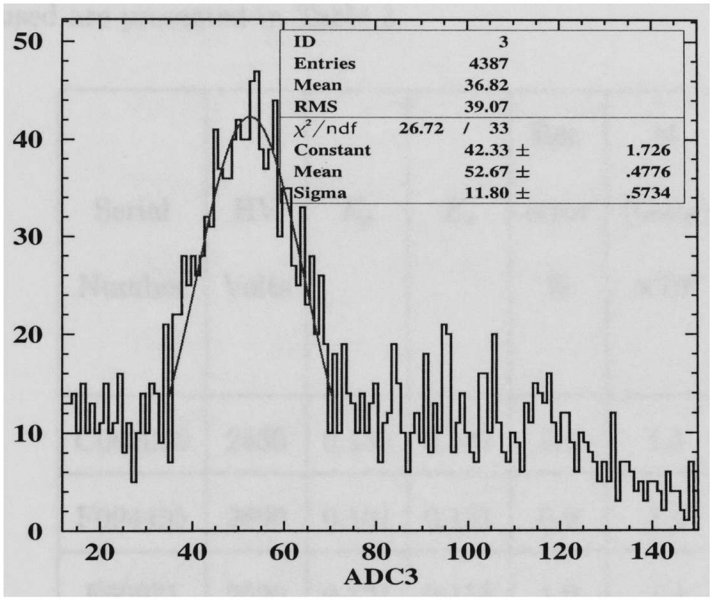

Figure 5: Gaussian fit to ADC spectrum for a Burle PMT – on the y axis is represented the number of counts and on x axis the ADC pulse height

[38] We fitted the ADC pulse height distribution, Poisson distributed, with a Gaussian since we are interested in the mean of the distribution only; the goodness of the fit, $\chi^2/ndgf$, tells us that this approximation is acceptable

[39] PMT's dark current, thermoionic emissions

To find out the starting channel taking into account the pedestal [40] position we used the formula:

$$N_{start} = N_{PED}\frac{Par(2) - N_{PED}}{3} \tag{41}$$

where N_{PED} is the pedestal position (the channel corresponding to the pedestal). The quantum efficiencies of the 24 PMT's determined using the above procedures and the high voltage used are presented in Table 2.

Serial Number	HV Volts	E_g	E_s	Rel. error %	M (Gain) $\times 10^8$
C065093	2430	0.135	0.181	2.1	1.1
F094495	2690	0.101	0.131	0.9	1.4
F69971	2520	0.121	0.158	1.9	1.1
F72592	2550	0.123	0.165	2.1	1.0
F73014	2550	0.124	0.164	1.9	1.1
J094787	2510	0.114	0.150	2.4	1.1
N27702	2600	0.203	0.242	1.8	1.2
N28245	2750	0.124	0.145	1.7	1.3
N32157	2650	0.126	0.163	1.9	1.1
N32515	2550	0.090	0.153	4.8	1.5
N32545	2500	0.111	0.141	1.9	1.1

[40] The charge obtained when a gate pulse is applied with no analog input

N32743	2500	0.120	0.150	1.9	1.1
N32746	2600	0.114	0.142	1.1	1.8
N90866	2420	0.137	0.176	1.8	1.2
N90872	2450	0.125	0.165	1.9	1.1
N93634	2520	0.118	0.148	0.8	1.6
T20703	2770	0.160	0.211	1.8	1.2
T21264	2500	0.131	0.172	1.8	1.2
T50026	2570	0.118	0.169	1.9	1.1
T50551	2560	0.147	0.194	1.8	1.1
T50676	2600	0.141	0.176	1.8	1.3
T50978	2450	0.170	0.196	1.8	1.1
U33859	2550	0.137	0.172	1.3	1.1
V026393	2670	0.101	0.140	2.1	1.1
V026395	2730	0.085	0.105	1.9	1.3
V26079	2500	0.123	0.149	1.6	1.3
Z016625	2430	0.128	0.171	1.8	1.1
Z40347	2610	0.129	0.163	1.5	1.1

Table 2: The PMTS' quantum efficiencies

The gains of the Burle phototubes were matched by adjusting the HV so that the anode current has an amplitude of 150 mV. Another gain matching was done using the software analysis PAW in order to obtain the ADC sum for all 24 PMT's. In Fig.

6 is shown one spectra of two PMT's before the software gain matching.

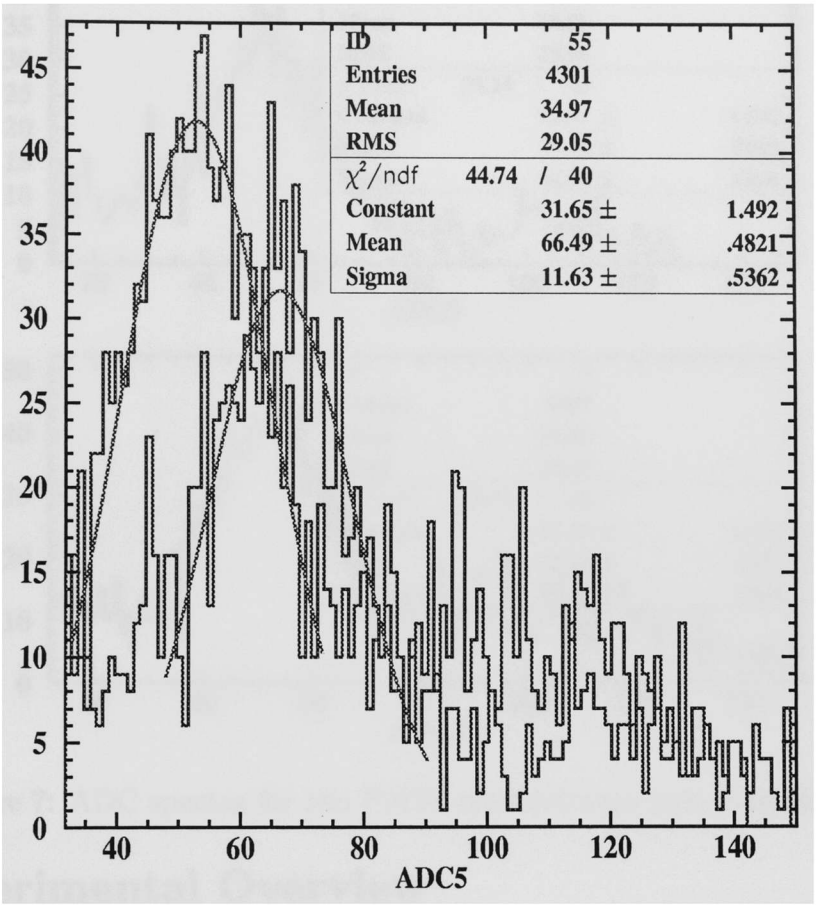

Figure 6: ADC spectra for two PMTs before software gain matching – on y axis is represented the number of counts and on x axis the ADC pulse height

Fig. 7 and Fig. 8 show the same spectra after the software gain matching. For simplicity we choose to illustrate only two PMT spectra (those with the greatest difference in gains).

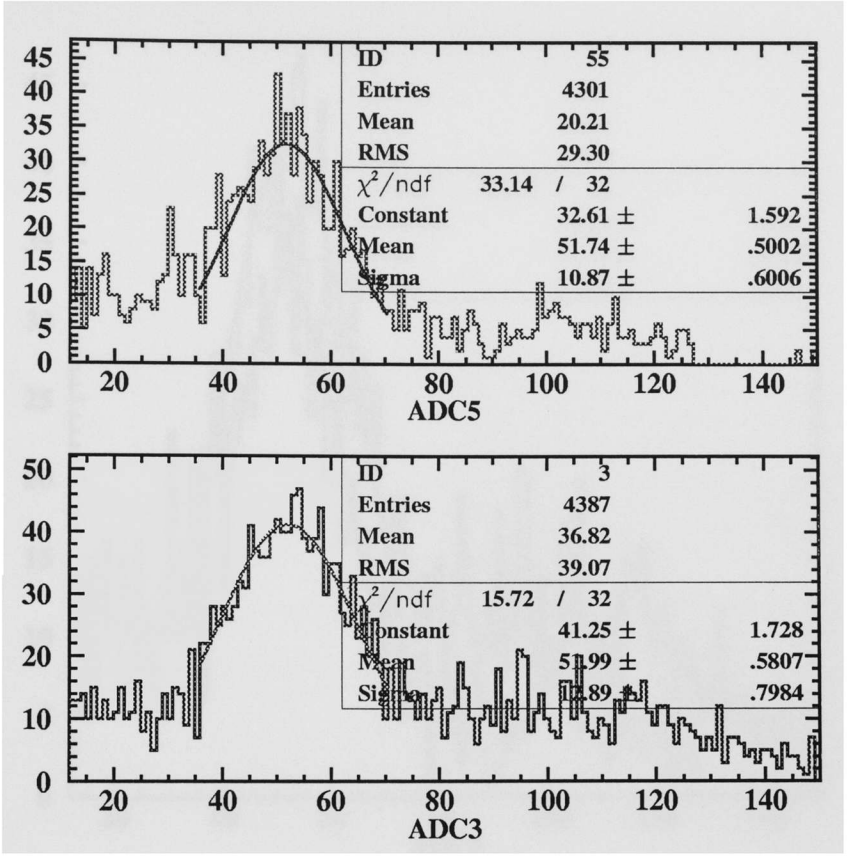

Figure 7: ADC spectra for two PMTs after software gain matching

3 Experimental Overview

The aerogel detector was installed in the hadron arm. For determining the efficiency for particles having velocities (relative to light speed) β above the relative threshold velocity β_t, the polarity of the magnets in the hadron arm was 'negative' to ensure that electrons are detected and hadrons (protons) are directed to the electron arm. The kinematics for opposite polarity of magnets ('+' in the electron arm and '−' in the hadron arm) used to measure the Aerogel counter's efficiency to particles above threshold is described in Table 3.

For determining the efficiency for particles having velocities (relative to light

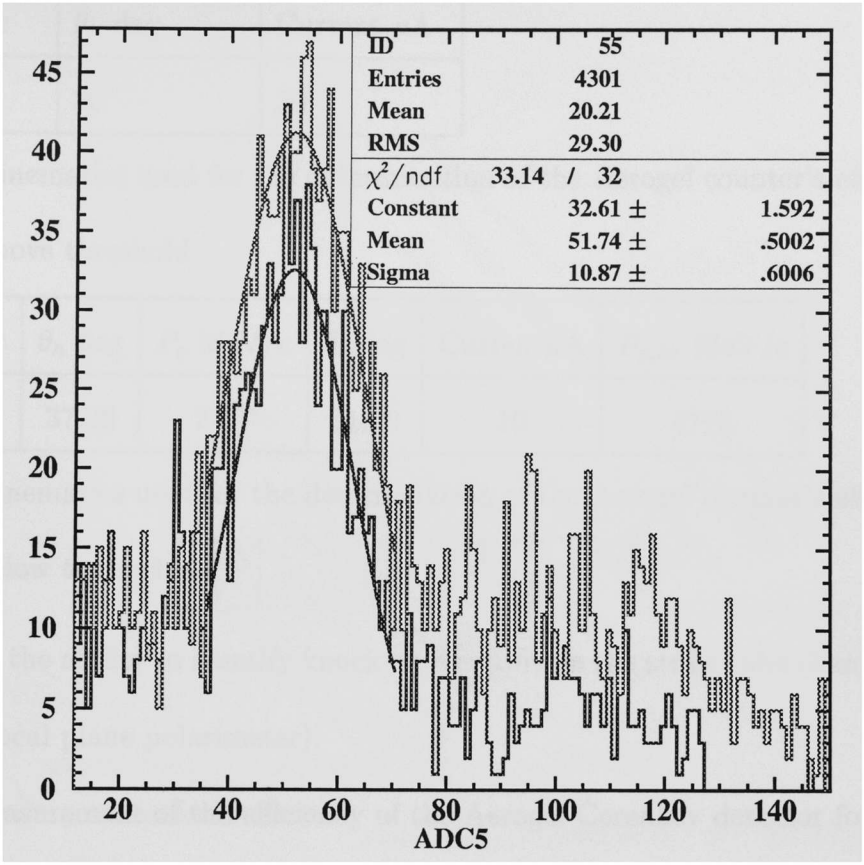

Figure 8: ADC spectra for two PMTs after software gain matching – on y axis is represented the number of counts and on x axis the ADC pulse height

speed) β below the relative threshold velocity β_t, the polarity of the magnets in the hadron arm was changed from '−' to '+'. The kinematics for normal polarity of magnets ('−' in the electron arm and '+' in the hadron arm) used to measure the Aerogel counter's efficiency to protons are described in Table 4.

Here β=0.9 means that the counter should (in the absence of knock-on electrons) never fire. The detected contamination for particles having beta below the threshold velocity come from accidental background (PMT dark current) and Čerenkov radiation produced by energetic knock on electrons (delta rays). This measurement

P_h MeV/c	θ_h deg	Current μA
2746	20	30

Table 3: Kinematics used for the determination of the Aerogel counter's efficiency to particles above threshold

P_h MeV/c	θ_h deg	P_e MeV/c	θ_e deg	CurrentμA	P_{pthr} MeV/c
1905.6	37.26	2177	31.99	10	4170

Table 4: Kinematics used for the determination of the Aerogel counter's efficiency to particles below threreshold

determined the ability to identify knock-on electrons in the straw tube chambers from the FPP (focal plane polarimeter).

The measurement of the efficiency of the Aerogel Čerenkov detector for particles above threshold and the rejection factor for subthreshold particles at momentum around 2 GeV/c was performed in Hall A at Jefferson Lab using an electron beam incident on a hydrogen target. The energy of the electron beam was 3.363 GeV. The set of measurements included single arm electron scattering, as well as the detection of electrons and protons in coincidence.

The rejection efficiency was determined at kinematics close to those of the kaon electroproduction experiments [41]. The first commissioning measurement was done with negatively charged particles (electrons implying β=1) to establish that the detector works. The Aerogel Čerenkov detector was placed in front of the focal plane polarimeter wire chamber and in between two scintillator detectors whose coincidence

[41] Experiment E98-108: Electroproduction of Kaons up to Q^2=3 $(GeV/c)^2$, Thomas Jefferson National Lab

was used to trigger the signal as shown in Fig. 9.

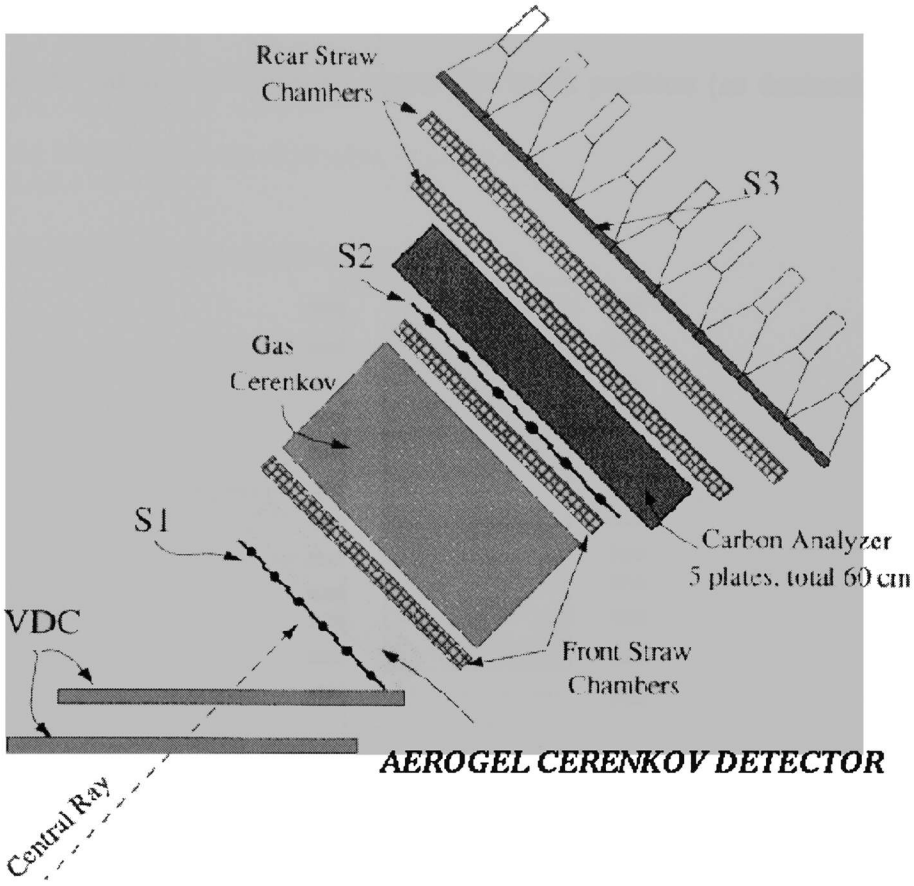

Figure 9: Hall A High Resolution Spectrometer Detector Package – Hadron Arm

For the second commissioning measurement [42] we used a ^{12}C target (the electrons being quasi elastic scattered off the carbon target) to cover the entire (a wider) region of the detector (although the detector was not uniformly illuminated). The protons' Fermi motion inside a ^{12}C nucleus smears the kinematics of the scattered electrons illuminating the detector more evenly.

The third commissioning measurement consisted in detecting the coincident elec-

[42] For the determination of aerogel detector efficiency to particles having velocities above the threshold required to produce Čerenkov radiation

trons and protons using the elastic $H(e, e'p)$ reaction. The Čerenkov counter had stacked in it aerogel pieces whose thicknesses were 3 and 9 cm as shown in Fig. 10. By plotting the number of photons versus the track position (as determined by the

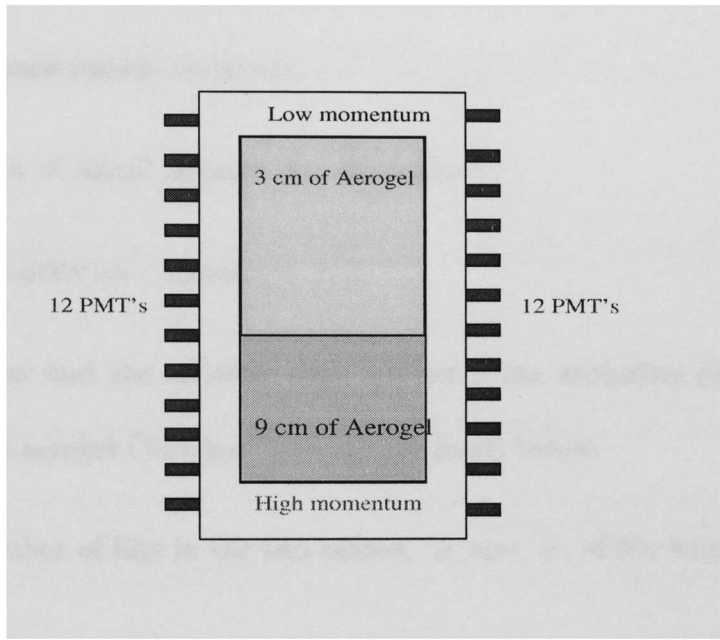

Figure 10: The Aerogel Čerenkov Detector showing aerogel position and channel layout

wire chambers extrapolated to the aerogel position), the effect of the aerogel thickness on the produced number of photoelectrons was measured. This measurement was done because the aerogel has a short optical scattering length leading to large attenuations. Although a thinner radiator yields fewer photons, it also scatters less so it was essential to establish the best thickness of aerogel given the scattering length and

the absorption length (the two processes that determine the number of photoelectrons produced by the Čerenkov radiation) for our index of refraction n=1.025.

In order to ensure a reliable data set from the phototubes the following items were checked before the commisioning experiment:

1. The PMTs' signals (anode currents);
2. The propagation of signal through the delay line [43];
3. The scintillator detectors' signal.

The logical conditions and the software cuts applied when analyzing data for the commissioning of the aerogel Čerenkov detector are listed below:

1. cuts on the number of hits in the two planes, 'u' and 'v', of the wire chamber;
2. cuts on angle of the particle track in the dispersive plane at the scattering point at the target;
3. cuts on angle of the particle track in the dispersive direction. The local central ray;
4. cuts on the number of clusters in the wire planes of the FPP wire chamber (the aerogel detector was placed in front of the FPP wire chamber);
5. a logical AND condition between the scintillator detectors placed one before and one after the aerogel detector (which determined a coincidence between the two detectors);

[43] By measuring the output of the delay lines with an osciloscope when a known pulse was sent to the input of the delay module

6. an AND logical condition between the clusters of the four planes u1,u2,v1,v2 of the wire chambers [44] ;

7. an AND logical condition between the non-dispersive position at the scattering point at the target [45] the clusters of the four planes u1,u2,v1,v2 of the wire chambers, the scintillator detectors and the number of reconstructed particle tracks [46];

8. cuts on the position in the Aerogel detector, to separately analyze the signal produced in the 3 cm / 9 cm region of the aerogel;

9. an AND logical condition between non-dispersive position at the scattering point at the target the clusters of the four planes u1,u2,v1,v2 of the wire chambers, the scintillator detectors and the number of reconstructed particle tracks;

10. an AND logical condition between the ADC sums for the two regions of the aerogel and the above 'good' variable.

The signals recorded and accepted for further analysis were the ones that fulfilled the above conditions. This means a signal that fired the desired block in the aerogel triggered by the two scintillators (in coincidence with each other) also fired the wire chamber and could be tracked back to the target (as being a signal produced by a particle that originated from a reaction in the target).

[44] i.e. 'good' signal in the wire chambers

[45] A 'good' event

[46] This was considered a 'golden' – analysable event

3.1 High Resolution Spectrometer Detector Package

The High Resolution Spectrometers in Hall A at Jefferson Lab consists of two magnetic systems and two detector packages. The role of the spectrometers is to select, record and identify particles emerging from a reaction in the target within a certain phase space in momentum and solid angle which defines the acceptance of the spectrometer.

The selection of a charged particle depending on its momentum is achieved by the curvature produced by the magnetic dipole field which is proportional to the particles' momenta.

The dipole field can be set up to obtain any central momenta values between 0.3 and 4.0 GeV/c. The path length of a particle entering the spectrometer system is 23.4 meters between target and detectors. The particle trajectory -central ray- is the reference for the symmetry plane of the spectrometer system. The magnetic system consists of three superconducting quadrupoles and one dipole. The quadrupoles determine the transverse focusing properties of the spectrometer and to a large extent its acceptance. The dispersive element in the system determines the central momentum of the spectrometer.

The hadron arm detector stack is illustrated in Fig. 9. It consists of two vertical drift chambers (VDC) that provide a precise measurement of the position and angle of incidence of both recoil electrons (in the HRS-E) and knockout protons (in the HRS-H) at the respective spectrometer focal planes. This information may be combined with the knowledge of the spectrometer optics to determine the position and angle of the particles in the target.

As charged particles pass through the chamber gas in the VDCs, they produce ionization. The ionized particles drift along the electric field lines defined by the high voltage planes and the signal wires. The charge is collected in the form of analog pulses on the signal wires. The pulses are then amplified, discriminated and used to start multihit TDCs, which are subsequently stopped by the overall event trigger. The TDCs are read out by CODA [47] (a software aquisition code). The data are displayed (histogramed) online by the DHIST software. In-depth offline data analysis required the ESPACE [46] software which was used for the determination of Aerogel Čerenkov detector efficiency. The High Resolution Spectrometer Vertical Drift Chambers provide a precise measurement of the position and angle of incidence of both recoil electrons (in the electron arm High Resolution Spectrometer – HRSe) and knockout protons (in the hadron arm High Resolution Spectrometer – HRSh) at the respective spectrometer focal planes.

This information may be combined with the knowledge of the spectrometer optics to determine the position and angle of the particles in the target. The detector stack contains also two planes of trigger scintillators S1 and S2 (see Fig. 9).

The plane of each scintillator array is perpendicular to the spectrometer central ray. The scintillator detectors are used to trigger the events of interest. The time necessary for a particle to travel the distance between the two scintillators allows the calculation of the speed of the particle. The Aerogel Čerenkov detector was placed in between the two scintillator detectors, connected in coincidence, which acted as triggers. If a particle passes through both scintillators within a fixed time

[47] Thomas Jefferson National Accelerator Facility, http://www.jlab.org

window the acquisition code was started and the event recorded. For the particles that triggered the scintillator detectors their track was determined with the Vertical Drift Chambers (VDC). The position where the charged particle interacted in the aerogel was determined with the VDC detectors.

4 Data Acquisition and analysis

The data analysis was conducted by using the computer package ESPACE for offline analysis, CODA for data acquisition and the Physics Analysis Workstation (PAW)[48] software from CERN as a graphical display and for the final data cuts. Standard statistical procedures were used to analyze the data: Gaussian and Poisson frequency distributions, and statistical error analysis. The algorithm used for calculating the yields for β_t=1 particles (electrons) consisted in defining the efficiency as the fraction of good electrons which gives a signal in the aerogel divided by the good electrons that did hit the Aerogel detector. The aerogel efficiency to detect a given particle as a function of the nuber of photoelectrons generated in the aerogel[49], was determined from the ADC sum spectra [50].

4.1 Aerogel Detector efficiency determination. Analysis results

The analysis results for the efficiency of the Aerogel Čerenkov detector to particles above/below the threshold relative velocity β_t, for the 9 cm layer of aerogel, as a function of the number of photoelectrons, is shown in Fig. 11.

The graphs indicate the probabilities of detecting a certain number of photoelec-

[48] http://wwwinfo.cern.ch

[49] A threshold was applied in the ADC to discard events producing less than a given number of phototelectrons

[50] The sum of the individual contributions of all PMTs

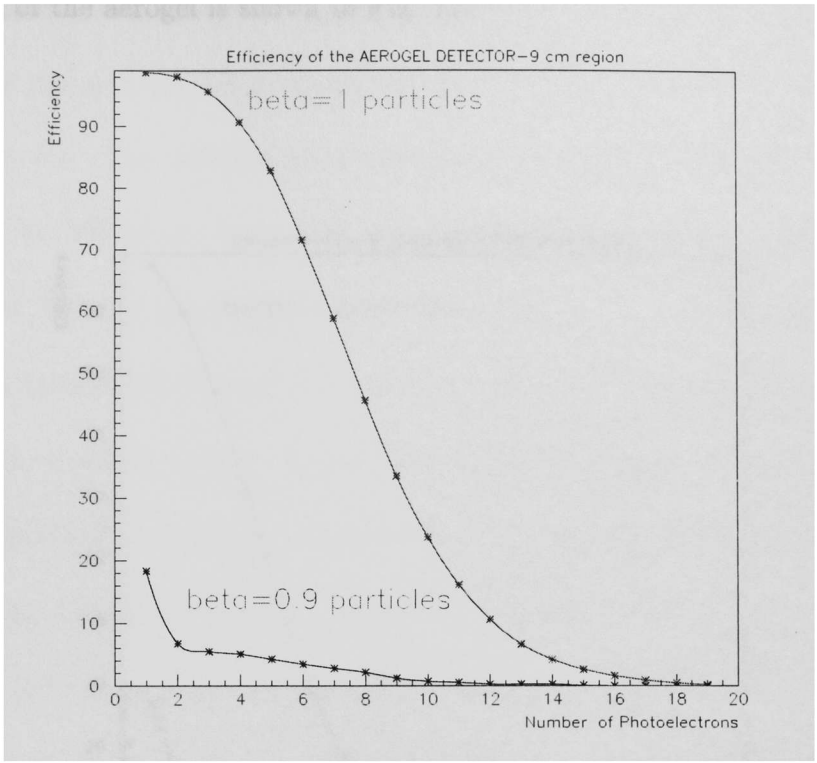

Figure 11: The Aerogel Čerenkov detector efficiency to particles having velocities above/below the threshold – 9 cm region

trons generated by particles above/below threshold, in the 9 cm region of aerogel. The probability of detecting 3 or more photoelectrons generated by particles above threshold was determined to be 95.58 % for the 9 cm region of the aerogel. For the same region of aerogel the probability of rejecting at least 3 photoelectrons generated by particles below threshold was determined to be 94.55 % The detection efficiency for β=0.9 particles was calculated by the ratio between the good protons, below the threshold velocity β_t, which gave a signal in the detector and the total number of good protons that hit the Aerogel detector.

The analysis results for the efficiency of the Aerogel Čerenkov detector to particles above/below the threshold β_t, as a function of the number of photoelectrons for the

3 cm region of the aerogel is shown in Fig. 12.

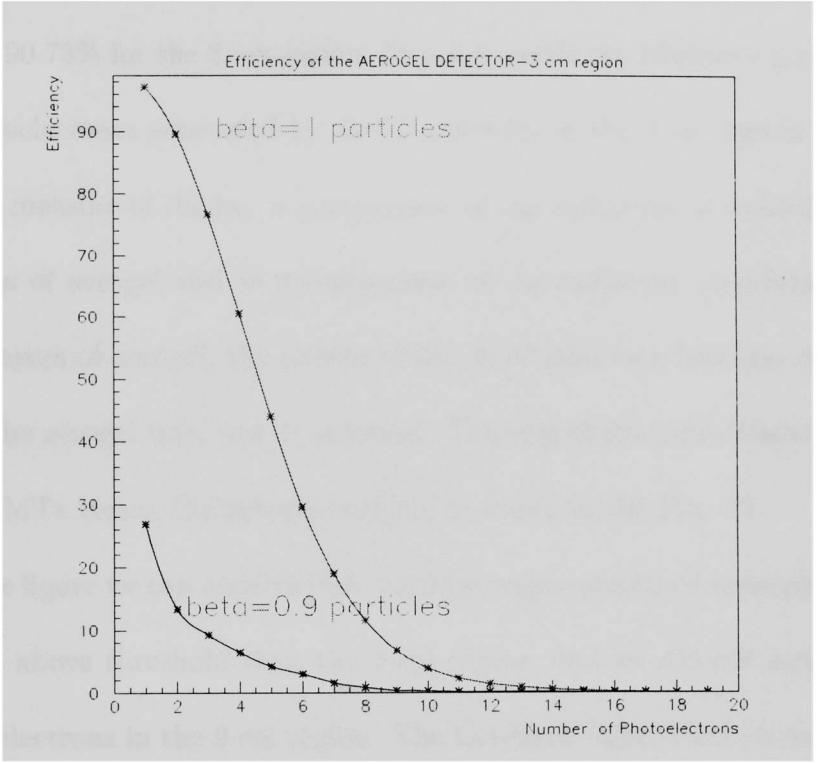

Figure 12: Efficiency of the Aerogel Čerenkov detector to particles above/below the threshold-3 cm region

The graphs indicates the probabilities of detecting/rejecting the required number of photoelectrons generated by particles above/below threshold, in the region of aerogel of 3 cm thickness.

The probability of rejecting at least 3 photoelectrons generated by particles below threshold (β_t=0.9756) was determined to be 90.73% for the 3 cm region of the aerogel. Thus efficiency for detecting at least 3 photoelectrons generated by β=0.9 particles in the 9 cm region of aerogel is 5.45%. The detection efficiency for β=0.9 particles was

calculated by the ratio between the good protons, below the threshold velocity β_t, which gave a signal in the detector and the total number of good protons that hit the Aerogel detector. The probability of observing at most 3 photoelectrons generated by β=0.9 is 90.73% for the 3 cm region. In other words the efficiency for detecting at least 3 photoelectrons generated by β=0.9 particles in the 3 cm region of aerogel is 9.27%. As a measure of the proportionality between the Čerenkov radiation yield and the thickness of aerogel and as a comparison of the radiation absorbtion coefficient in the two layers of aerogel, the results of the ADC sum as a function of the aerogel position in the aerogel tray, was determined. The sum of the pulse height distribution for the 24 PMTs versus the aerogel position is shown in the Fig. 13.

From the figure we can observe that the 9 cm region produced more photoelectrons for particles above threshold than the 3 cm region, and we did not generate 3times more photoelectrons in the 9 cm region. The Čerenkov light is not strongly absorbed by the additional 6 cm of aerogel.

The result of this analysis and the presence of the Aerogel Čerenkov detector were used togheter with a time of flight spectra [51] to obtain a missing mass spectrum for the H(e,e'K)Y reaction. The missing mass spectra was analysed in two cases: with a software cut in the aerogel [52]and without the software cut. The result of analysis is presented in Fig. 14 without the cut applied on the Aerogel detector and in Fig. 15 with the cut applied on the Aerogel detector.

From the graph one can conclude that the presence of the Aerogel detector yields

[51]The time needed for particles to travel from target to the detectors

[52]The software cut means we rejected all events recorded by the aerogel detector, all the pions that generated photoelectrons

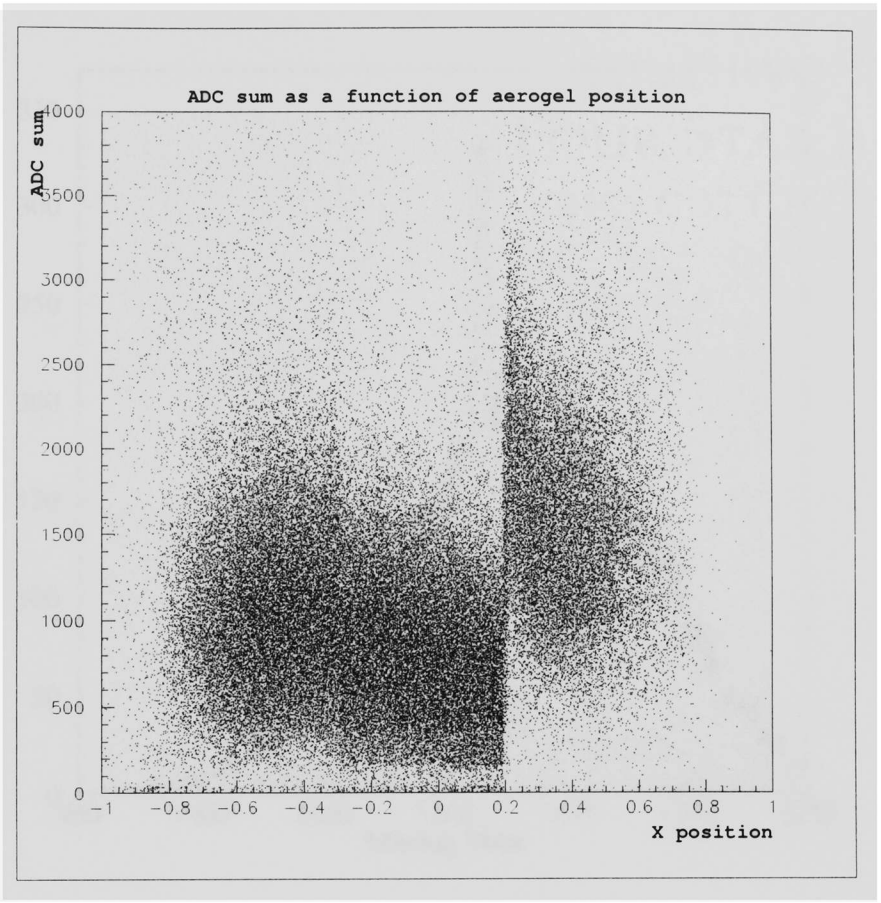

Figure 13: ADC sum as a function of the aerogel position

a clean missing mass spectrum allowing a more accurate identification of the Λ and Σ hyperons [53] and implicitly of the strangeness particle (the Kaon) through the rejection of contaminating particles (π).

[53]The left picture has a big background due to coincident pions and the Σ peak is hidden underneath the pions' peak; in the right picture we can clearly distinguish the Σ peak from π background

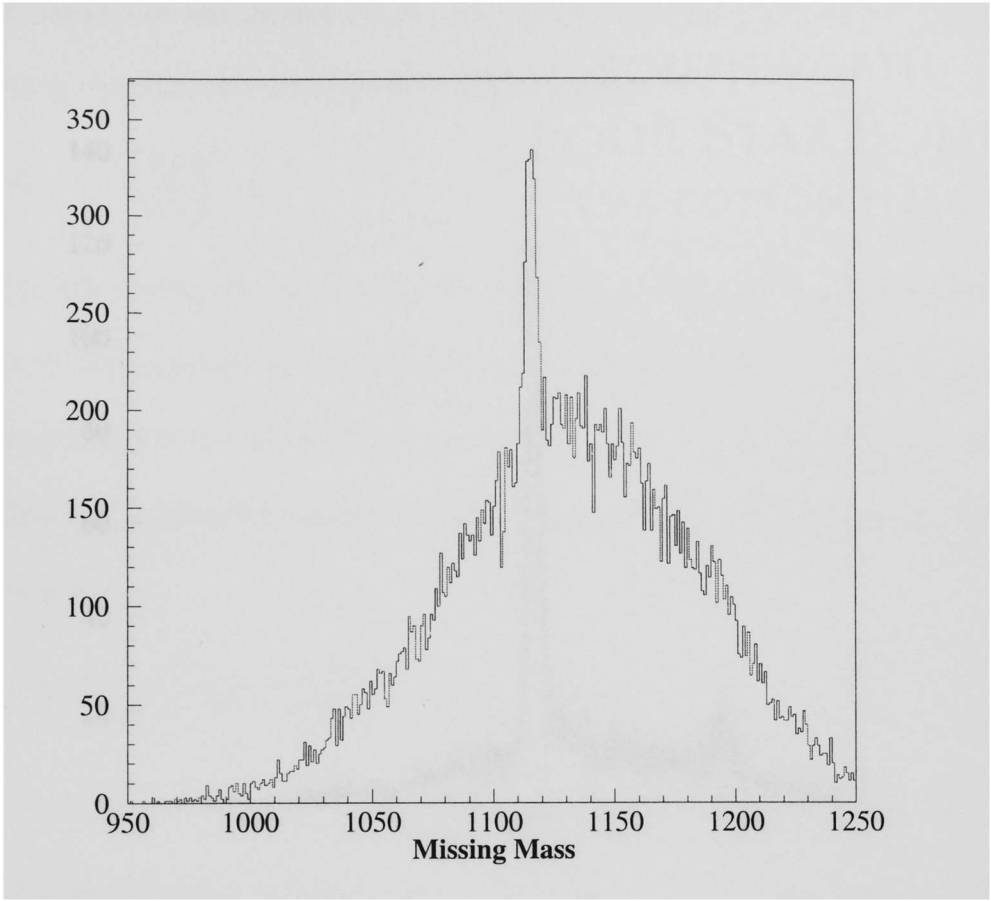

Figure 14: Missing mass spectrum (Λ hyperon at 1115.7 MeV/c^2) without the cut applied on the Aerogel detector

5 Error analysis

The error analysis performed on the Aerogel Čerenkov detector's efficiencies included systematic and statistical errors. The result of the error analysis implies that systematic errors are dominant. The statistical errors account for no more than 10% of the systematic errors in the case of efficiencies for particles above threshold and between 19 % and 60 % for the rejection factors [54]. We used the Gaussian distribution

[54]The comparison of the systematic and statistical errors indicated are for generating up to 6 photoelectrons in the detector

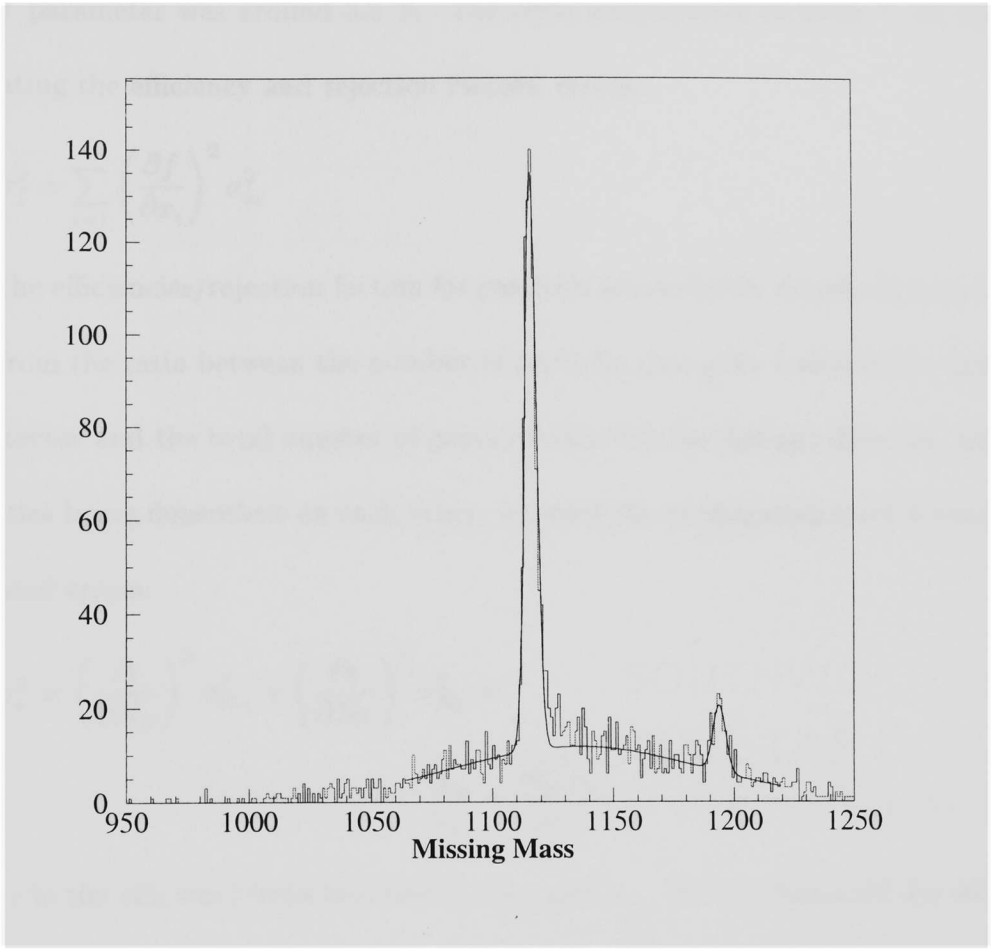

Figure 15: Missing mass spectrum (Λ hyperon at 1115.7 MeV/c^2 and Σ^0 at 1192.6 MeV/c^2) with the cut applied on the Aerogel detector

function[55] [56]:

$$f(x;\mu,\sigma^2) = \frac{1}{\sigma\sqrt{2\pi}} e^{-\frac{x-\mu^2}{2\sigma^2}} \tag{42}$$

to fit the ADC spectra for each phototmultiplier and the ADC sum spectra. The goodness of fit statistics were given by the χ^2 parameter per degree of freedom (χ^2/ndf [57]). As one can see from the fitted spectra, Figures 7 and 8, the relative error of the

[55] μ the mean of the distribution, and σ the standard deviation

[56] Review of Particle Physics, C, Vol. 15, Springer, 2000

[57] The number of degrees of freedom is the difference between the number of bins of the distribution and the number of free parameters which are allowed to vary

χ^2/ndf parameter was around 3.5 %. The error propagation formula [58] we used in calculating the efficiency and rejection factors' errors:

$$\sigma_f^2 = \sum_{i=1}^{n} \left(\frac{\partial f}{\partial x_i}\right)^2 \sigma_{x_i}^2 \tag{43}$$

Since the efficiencies/rejection factors for particles above/below threshold were calculated from the ratio between the number of particles that gave a recordable signal in the detector and the total number of particles that hit the Aerogel detector, the two quantities being dependent on each other, we used the propagation error formula for correlated errors:

$$\sigma_\epsilon^2 = \left(\frac{\partial \epsilon}{\partial N_G}\right)^2 \sigma_{N_G}^2 + \left(\frac{\partial \epsilon}{\partial N_T}\right)^2 \sigma_{N_T}^2 = \tag{44}$$

$$= \frac{\sigma_{N_G}^2}{N_T} + \frac{\sigma_{N_T}^2 \epsilon_G}{{N_T}^2}$$

where ϵ is the efficiency/rejection factor, σ_{N_T} and σ_{N_G} are the standard deviation of the number of particles that hit the detector respective the number of particles that 'fired'[59] the detector. The calculated statistical errors for the rejection factors ranges from 1.9 % to 5.8 % for the 9 cm region and from 1.5 % to 6.4 % for the 3 cm region as we can see from the Table 5. The calculated statistical errors for the Aerogel detector efficiencies ranges from 0.5 % to 1.3 % for the 9 and 3 cm region (see Table 5)[60].

N_{PE}	$\epsilon_{\epsilon_p}^{9cm}$ (%)	$\epsilon_{\epsilon_p}^{3cm}$ (%)	$\epsilon_{\epsilon_e}^{9cm}$ (%)	$\epsilon_{\epsilon_e}^{3cm}$ (%)
1	1.9	1.5	0.5	0.5

[58] Review of Particle Physics, C, Vol. 15, Springer, 2000

[59] i.e. emitted light in the detector

[60] The ranges in relative errors for efficiencies/rejection factors indicated are for generating up to 6 photoelectrons in the detector

2	3.5	2.2	0.5	0.1
3	4.1	2.8	0.5	0.1
4	4.3	3.7	0.7	0.1
5	5.0	5.0	0.9	0.2
6	5.9	6.4	1.3	0.2

Table 5: The Relative errors for Aerogel detector' efficiencies

In Table 5 $\epsilon_{\epsilon_e}^{xcm}$ is the relative error of the efficiency for detecting particles above threshold in the x cm region of aerogel and $\epsilon_{\epsilon_p}^{xcm}$ is the relative error of the efficiency for detecting particles below threshold in the x cm region of aerogel. We did not include the efficiencies of the wire chamber and scintillator detectors in the error calculation because in the formula considered these errors would appear at both denominator and numerator so they cancel out. The systematic errors considered in the error analysis came from the PMTs' gain matching procedure described in chapter 3. In order to perform the described software gain matching, an optimised database file containing the gains and pedestal positions was used and read by the ESPACE analysis code. A comparison between the optimised database file used for our analysis and a database that used a different optimisation [61] resulted in an estimate of a systematic error of 10 %. In our analysis we calculated that a photoelectron peak corresponds to 200

[61] Bogdan Wojtsekhowski, Thomas Jefferson National Lab., technical report

channels of the ADC, whereas with the optimised database file from the cited article a photelectron peak corresponded to 190 channels. Thus in our analysis we were off by 100 channels (0.5 photoelectrons) for each 2000 channels (10 photoelectrons). Therefore the systematic errors account for 10 % and are almost twice as big as the statistical errors.

6 Conclusions

The technique used to calculate the aerogel detector's efficiency was based on the detection of Čerenkov radiation. For this study we used the detector package of Hall A in Jefferson Laboratory. The probabilities of obtaining a certain number of photoelectrons generated by above threshold particles was determined using the quasielastic reaction C(e,e'), the electron being scattered off of a carbon target to cover a wider area of the detector. The detection of the contamination for particles having β below the threshold velocity was measured using the H(e,e'p) elastic reaction. The contamination coming from accidental background (PMT dark current) and Čerenkov radiation produced by energetic knock-on electrons (delta rays) was also measured and studied. The sub-threshold particles cannot generate Čerenkov radiation in the detector but they knock-out the atomic electrons that have enough energy to generate the radiation.

From the comparative analysis results of the two regions of aerogel one can conclude that the 9 cm region has a greater efficiency for the particle having velocities above threshold and a greater rejection factor for the contaminanting particles (sub-threshold particles). The rejection efficiency was determined at the kinematics close to those of the kaon electroproduction experiments. From the sum of the pulse height distribution of the ADC versus the position of the aerogel in the detector we determined that the amount of light generated is proportional to the thickness of aerogel and that the Čerenkov light is not strongly absorbed by aerogel; corroborating these results with the previous ones determined the choice of an aerogel layer of 9 cm for the Aerogel Čerenkov detector.

The influence of the aerogel's short optical scattering length on the attenuation process was studied by plotting the number of photoelectrons versus the track position (as determined by the wire chambers extrapolated to the aerogel position).

The coincidence Time-of-Flight spectra with a cut applied on the aerogel was used together with the analysis of the rejection of background events in order to yield clean missing mass spectrum as shown in Fig. 15. The cut on the aerogel was applied to obtain two photoelectrons or more in the entire diffusion box. The cut was applied to discard the knock-out electrons having energies very close to threshold.

This was a conclusive analysis which proves that the Aerogel diffusion detector achieves the particle identification required by the experimental program.

LIST OF REFERENCES

1. Leo, William R., Techniques for nuclear and particle physics experiments, 1994

2. P. Carlson et al., Nuclear Instruments and Methods 160/1979

3. Arlon J. Hunt, Aerogel optical properties and spectrum, http://rd11.web.cern.ch

4. Jim Napolitano,Thomas Jefferson National Lab., technical report, http://www.jlab.org

5. BURLE TECHNOLOGIES, INC., http://www.burle.com

6. Sparrow Corporation, http://sparrowcorp.com

7. Review of Particle Physics, C, Vol. 15, Springer, 2000

8. Bogdan Wojtsekhowski, Thomas Jefferson National Lab., technical report

9. Konrad Kleinknecht, Detectors for particle radiation, Cambridge Univ. Press, 1998

10. J. D. Jackson, Classical Electrodynamics, Wiley, New York, 1996

11. LeCroy, http://www.lecroy.com

12. CERN-European Laboratory for Particle Physics, http://wwwinfo.cern.ch

13. Thomas Jefferson National Accelerator Facility, http://www.jlab.org